Clinical application of CSF flowmetry in various neurological conditions

Norhan Mohamed Helmy, Faten Fawzy Mohammed Hafez, Mohamed Ashraf Zaitoun, Riham Dessouky

Radiodiagnosis Department, Faculty of Medicine- Zagazig University, Egypt

Email: helmynoran@gmail.com

Article History: Received 10th June, Accepted 5th July, published online 10th July 2023

Abstract

Much of our understanding of the hemo-/hydrodynamics relating to CSF flow has come from Phase Contrast Magnetic Resonance Imaging (PC-MRI) experiments. PC-MRI uses the change in the phase of the MR signal, which occurs when fluid (such as blood or CSF) flows in a static magnetic gradient. This phase change is proportional to the fluid's velocity. PC-MRI is a technique that provides qualitative and quantitative assessment of a moving fluid; thus, study of the CSF flow became one of its major applications. The keystone of PC-MRI is a bipolar gradient i.e., a gradient with the same positive and negative magnitude and the same application time of both. This bipolar gradient is placed in a sequence after the radiofrequency pulse and before data collection during echo time (TE). If the bipolar lobe is applied only in one axis, the gradient sensitises the image to the flow in just one direction. Knowing that, the application of a bipolar gradient in all three axes is necessary to develop a sequence sensitive to flow regardless of the direction. Phase-contrast MRI can be used for quantitative assessment of CSF flow, in which measurements such as flow velocity and volume are used to diagnose conditions and direct care in the appropriate patients. In addition, phase-contrast MRI enables qualitative assessment of CSF circulation (ie, bulk flow) and back-and forth motion (ie, pulsatile flow). One of the most widely used applications of CSF flow imaging is functional assessment of normal pressure hydrocephalus (NPH). Hyperdynamic flow of CSF is seen when there is enlargement of the ventricular system in the absence of or out of proportion to the sulcal enlargement (ventriculosulcal disproportion). Patients with NPH who have hyperdynamic CSF flow respond better to ventriculoperitoneal shunt placement than do patients with normal or decreased flow.

Keywords: CSF flowmetry, neurological conditions

DOI: 10.53555/ecb/2023.12.Si12.234

Much of our understanding of the hemo-/hydrodynamics relating to CSF flow has come from Phase Contrast Magnetic Resonance Imaging (PC-MRI) experiments. PC-MRI uses the change in the phase of the MR signal, which occurs when fluid (such as blood or CSF) flows in a static magnetic gradient. This phase change is proportional to the fluid's velocity. PC-MRI is a technique that provides qualitative and quantitative assessment of a moving fluid; thus, study of the CSF flow became one of its major applications. The keystone of PC-MRI is a bipolar gradient i.e., a gradient with the same positive and negative magnitude and the same application time of both. This bipolar gradient is placed in a sequence after the radiofrequency pulse and before data collection during echo time (TE). If the bipolar lobe is applied only in one axis, the gradient sensitises the image to the flow in just one direction. Knowing that, the application of a bipolar gradient in all three axes is necessary to develop a sequence sensitive to flow regardless of the direction ***(1).***

The principle of the bipolar gradient is to develop a phase shift of spins moving with a specific velocity along the direction of the axis, where spins moving in the direction of the bipolar gradient acquire a positive net phase shift (represented as white colour in the phase images of PC-MRI), while spins moving in the opposite direction to the gradient acquire a negative net phase shift (represented as black colour in the phase images

of PC-MRI). The amount of acquired net phase shift is directly proportional to the flow velocity and time of bipolar gradient application (in range from 0 to +φ or –φ). This explains the significance of choosing a proper velocity parameter – velocity encoding (VENC) – that is matched by the magnitude and width of the bipolar gradient ***(1).***

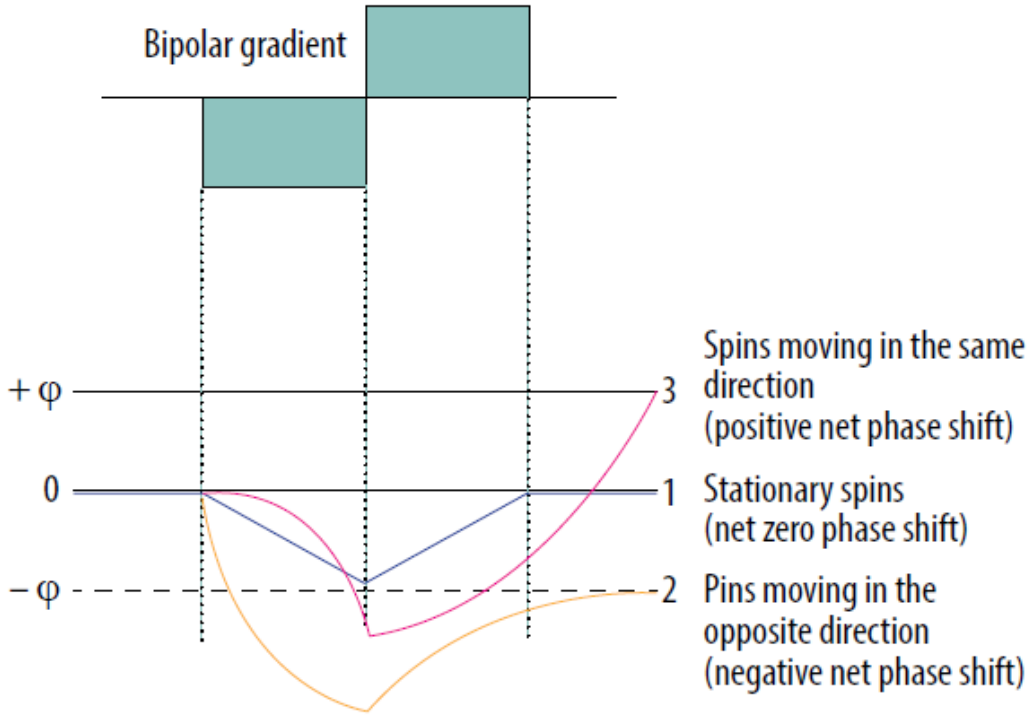

Figure ; 1. Phase shift during the application of bipolar gradient. 1. Stationary spins (blue line) acquire the same amount of negative phase shift and positive phase shift as the bipolar gradient is applied. 2. Spins moving in the opposite direction (yellow line) acquire negative phase shift because they are more prone to negative lobe of the bipolar gradient – they are more exposed to a higher magnetic field in the opposite direction. 3. Spins moving in the same direction (pink line) acquire higher positive phase shift as the positive lobe of the bipolar gradient is applied – they are exposed to the increased magnetic field with the direction of the flow ***(2).***

Stationary tissue spins obtain the same amount of negative phase shift from a negative lobe of the bipolar gradient, and positive phase shift from the positive lobe. Lack of any motion throughout the acquisition, i.e., staying in one location and experiencing the same amount of gradient pole strength in opposite directions, results in a zero net phase shift. Each time, the PC-MR sequence must take an additional set of images without any bipolar gradient applied (reference images), to subtract data from the velocity encoded image. Only the signal of stationary spins is identical in both sets of images and is subtracted. This results in an image with the signal only from flowing spins. ***(2).***

A crucial parameter of every PC examination is VENC, which is directly connected with the properties of the bipolar gradient. The magnitude defines the maximum positive (+φ) and negative (–φ) range of phase change. Underestimating the VENC value (fluid has higher velocity than assumed) leads to aliasing artifact. For that reason, it is strongly advised that a VENC is selected at slightly above the mean velocity of the investigated fluid. A typical velocity encoding value is 10 cm/s for CSF traversing through the foramen magnum and 8 cm/s for CSF traversing through the cerebral aqueduct. In some pathological conditions, e.g., in aqueduct stenosis, it may be necessary to select VENC higher than normal because of the higher velocity through the stenotic area. However, overestimation of velocity encoding leads to a low signal acquired from the flow and a low-signal to-noise ratio (SNR). ***(2).***

Phase-contrast MR images consist of magnitude and phase images. The magnitude image represents flowing CSF visualised as a bright signal, while stationary tissues are supressed, shown as a black background. The phase image is phase-shift encoded (through-plane or in-plane), with white signal and black signal representing forward and backward flows, respectively. Being phase-dependent, it comprises the velocity information, which can be quantitatively estimated **(3).**

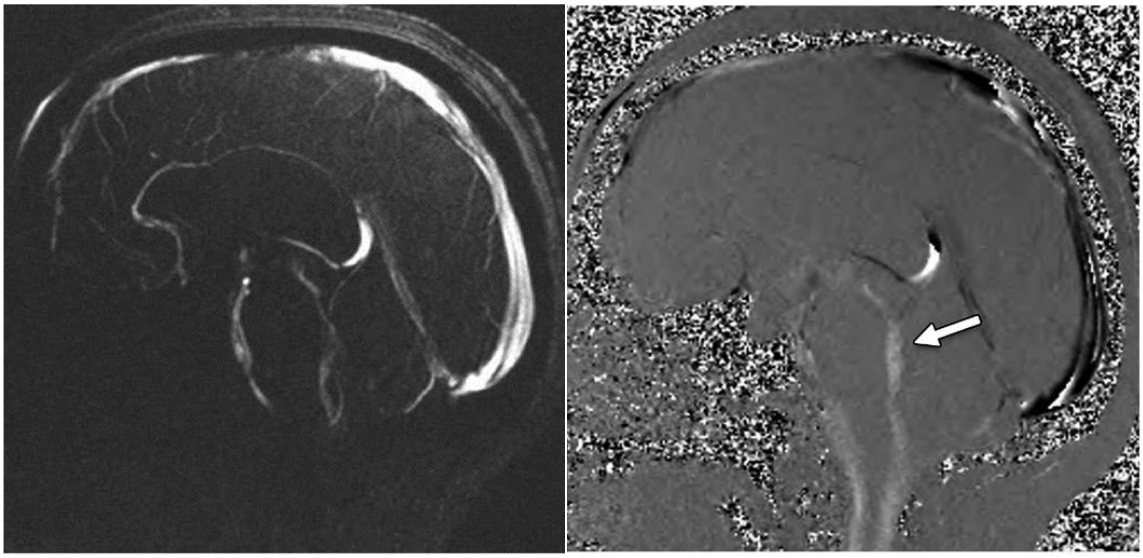

a. b.

Figure 2. Magnitude (A) and phase (B) images. The magnitude image – flow is represented as bright signal, while stationary tissues are shown as a black background (signal is suppressed). The phase image – direction of the flow is encoded due to phase shift of flowing spins. The forward flow is represented as a bright signal, contrary to the reverse flow represented as a dark signal **(3)** mid grey .

Pulsatile CSF flow can be displayed in both type of images, thanks to PC-MRI gating with the cardiac cycle. A prospective or retrospective gating must be performed, to map pulsatile flow data on heart action and to increase the signal-to-noise ratio. As has been proven, the retrospective gating, based on assigning and averaging the signal to specific cardiac phases, is more reliable than the prospective one Likewise, PC-MRI sequence acquire signal from a few minutes of flow, which is averaged and plotted in relation to cardiac phases. CSF flow during the cardiac cycle may be displayed as the cine loop. Phase-contrast MRI as a method of flow imaging that is not free of limitations and pitfalls. First, quantitative assessment of mean peak velocity, peak systolic velocity and stroke volume is possible only in one plan exactly perpendicular to the unidirectional flow (jets), to prevent a partial volume effect. Evaluation of a multidirectional flow that could be objectively calculated in multiaxial planes is out of reach in 2D and 3D phase-contrast MRI– this is why this technique is not useful for assessment of the flow inside subarachnoid cysts, the reflux flow from the third ventricle to lateral ventricles, or other types of turbulent flow ***(4)***.

Secondly, methods of manual segmentation (instead of semi-automated techniques) and manual region of interest (ROI) placement are responsible for interobserver and variability in the collected data. A size of the ROI affects stroke volume, flow rate, and mean velocity values. Only peak flow velocity is ROI-independent. However, acceptable repeatability and sufficient accuracy were proven, and only discrete changes in data were detected due to the mentioned reasons. Stroke volume was also established as very accurate and least variable in the case of patients with NPH. Plane selection in relation to the anatomic region of the aqueduct may also affect the overall obtained values, but these inequalities were found to be insignificant based on healthy volunteers ***(4)***.

Figure 3. Flux curve and parameters of flow derived from the phase-contrast images. Region of interest (ROI) was placed in the perpendicular intersection of the aqueduct (red arrow). Images were acquired with velocity encoding value (VENC) = 12 cm/s. The flux curve represents the flow plotted against cardiac cycle. The values were obtained and calculated from the ROI. Several parameters can be calculated from the selected ROI. Stroke volume, mean velocity and peak velocity are mostly used for quantitative comparison, with the stroke volume being the most comprehensive ***(2).***

Nevertheless, PCMRI remains the most evaluated and the most frequently used technique and the only quantitative method to date. A proper velocity encoding value (connected with Vmax of flowing spins, which is rephased with the bipolar gradient) is necessary, to receive the highest signal possible. It is recommended that values of velocity encoding are selected slightly higher than the expected velocity of the examined fluid. Nonetheless, overestimated VENC leads to a diminished signal; on the other hand, underestimated VENC leads to the aliasing artefact – commonly present in the centre of the vessels, where flow velocity is higher than anticipated. It causes a phase shift greater than $+\pi$ or $-\pi$. Spins exceeding the range of velocity encoding are going to wrap back simulating the flow in the opposite direction.

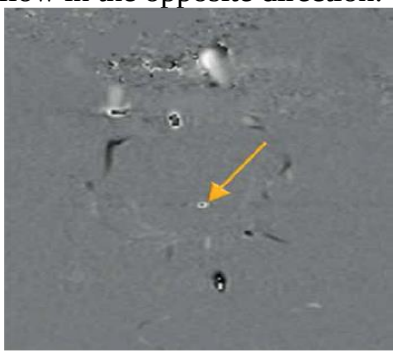

Figure 4. Aliasing artefact in the phase image (yellow arrow). Flow velocity in the center of the aqueduct is higher in comparison to selected velocity encoding values. Underestimation of velocity encoding leads to incorrect mapping of the flow in the centre, as a flow in the opposite direction (black point)**.** ***(2).***

High quality PC-MR images are dependent on fine tuning between VENC, TR, and SNR. Sensitizing an image to 5-8 cm/s CSF flow requires usage of strong bipolar gradients. The slower the velocity encoding, the stronger the magnitude that must be applied for a longer time, thus increasing TR. On the other hand, TR

cannot be indefinitely increased; a relatively short repetition time is necessary to achieve maximal temporal resolution because the data must be plotted against one full cardiac cycle. Therefore, rigorous selection of proper sequence parameters is fundamental ***(5)***.

Electrocardiogram or finger plethysmography are used to plot data over the phases of the cardiac cycle. All the data are averaged from each cycle through the whole sequence, displayed as one cine loop. This is why the PC-MRI is insensitive to dynamic changes in CSF flow and turbulent flow, and insensitive to respiratory-derived CSF motions, because it represents an average from one time window ***(4).*** Undoubtedly CSF PC-MRI is a leading method for quantifying CSF flow velocities (such as stroke volume, peak systolic velocity, mean systolic volume, etc.) in different anatomical locations (sylvian aqueduct, foramen magnum) for clinical requirements such as differential diagnosis (e.g. NPH, Chiari type I, syringomyelia), postsurgical follow-up (patency of ventriculostomy, shunts, etc.), and it remains a promising, significant, and accessible MRI sequence (**6)**

1. Parameters of CSF Flow

a. Cine / qualitative measurements:

1. In normal subjects with a patent aqueduct, the downward flow of CSF is maximally shown 175 to 200 ms after the R wave of electrocardiogram. This caudal flow of CSF through aqueduct is preceded by outflow of CSF from fourth ventricle via the foramen of magendie in the sagittal plane**.** In the middle of the cardiac cycle a rostral wave of CSF is seen as a reverse pulse through the aqueduct. Between these pulses, no fluid motion is detected. Normally some degree of flow can be appreciated in the posterior third ventricle, foramen of monro and rostral and caudal fourth ventricle. CSF pulsations can be seen in basal cisterns but not in the lateral ventricles **(7) .**

b. Phase / quantitative measurements:

Phase measurements can show bidirectional flow of CSF and velocities of flow can be measured. Phase images are usually obtained in the axial plane (perpendicular to the aqueduct of Sylvius. Since the aqueduct normally measures 2-3 mm, the slice thickness of 5-6 mm causes volume averaging and results in lower calculated CSF velocity than the actual velocity (volume averaging of static material within a given voxel). Caudal aqueductal CSF flow velocities of 3.7 to 7.6 mm/ sec have been measured in normal subjects**.** Average aqueductal flow rate values less than 18mL/min are considered normal in elderly patients ***(8)***.

Quantitative CSF flow parameters

Several CSF flow parameters may be calculated by flow analysis software; however, the most used CSF flow parameters are CSF stroke volume, peak systolic velocity (PSV) and peak mean velocity. Each parameter is defined as follows.

i. **Stroke Volume** : The average of the volume passing backward & forward (during systole & diastole) together and the divided into 2 .
ii. **Peak systolic velocity (PSV**) : is the maximal velocity in any pixel of the ROI during systole.
iii. **peak mean velocity**: (the peak of the average velocities in all pixels of the ROI).

Table 1 summarizes the normal range of aqueductal peak velocities and flow in adult patients (9):

Flow Parameters	Range	Mean
Peak systolic velocity (cm/sec)	**2.59 – 8.63**	**5.56**
Peak end-diastolic velocity (cm/sec)	**2.4 – 9.26**	**4.73**
Systolic mean flow (mL/min)	**0.6-14.4**	**3.6**
Systolic stroke volume (microliter)	**4-115**	**28**

Pathophysiology and role of MRI in assessment of ventriculomegaly/ hydrocephalus

1. Pathophysiology of hydrocephalus:

Hydrocephalus is one of the complex and multi-factorial neurologic disorders. The mechanism of hydrocephalus is nearly always obstruction somewhere along the CSF pathways. A formation/absorption mismatch also results in an increase in the CSF volume within the ventricles and/or subarachnoid spaces. Finally, an increased production of CSF by choroid plexus tumors is also a rare cause of hydrocephalus ***(10).*** Hydrocephalus may be classified as acute or chronic, compensated or uncompensated, normal-pressure or high-pressure, communicating or non-communicating in nature. Acute and chronic refers to the time course. In acute hydrocephalus, there is a time course of days or weeks with symptoms of high intracranial pressure. In chronic hydrocephalus, the findings have been present for months or years. Active, compensated, or arrested refers to whether hydrocephalus is still producing symptoms. Normal-pressure or high-pressure refers to the CSF pressure ***(11)***

A more commonly used classification is communicating or non-communicating, according to whether there is a normal communication between the ventricular system and subarachnoid space. This distinction was based traditionally (but no longer in practice) on whether dye injected into the lateral ventricles could be detected in CSF withdrawn by lumbar puncture ***(10).*** Non-communicating hydrocephalus tends to demonstrate higher CSF pressures and a more rapid rate of ventricular enlargement, requiring more urgent investigation and treatment while communicating hydrocephalus tends to be less rapid in its course ***(12)***.

2. Classification of Non-Tumoral Hydrocephalus

The Japanese "Research Committee on Intractable Hydrocephalus" classified non-tumoral hydrocephalus into eight types, based on the etiology and time of onset of hydrocephalus (**13):**

- **Hydrocephalus Seen Mainly Early in Life**

1- Fetal hydrocephalus
2- Infantile congenital hydrocephalus
3- Hydrocephalus associated with dysraphism
4- Post-hemorrhagic hydrocephalus in premature neonates
5- Post-meningitic hydrocephalus

- **Hydrocephalus Seen Mainly in Adults**

1- Hydrocephalus following sub-arachnoid hemorrhage
2- Idiopathic adult hydrocephalus or normal-pressure hydrocephalus
3- Post-traumatic hydrocephalus

Role of MRI in assessment of hydrocephalus

a. MRI Criteria of Hydrocephalus

i. Early dilatation and rounding of the temporal horns:

This may be the earliest manifestation of ventricular obstruction and may be seen before obvious enlargement of the bodies of the lateral ventricles. On the other hand, temporal horn dilatation as a manifestation of temporal lobe atrophy occurs later ***(14).***

ii. Periventicular edema:

This finding is seen especially in the periventricular white matter of the frontal horns in acute and sub acute phases of hydrocephalus (high-signal halo on T2-weighted images, FLAIR and Proton density image sequences).

Fig (14): Axial FLAIR MR shows dilatation of the temporal horns (arrow) and Periventricular hyper intensities representing peri ventricular edema (black arrows) ***(14).***

iii. Enlargement and ballooning of the third ventricle:

In atrophy the third ventricle tends to enlarge by increasing the distance between its walls, which tend to remain parallel to each other. Ballooning and rounding of the third ventricle are characteristic of hydrocephalus. In the sagittal projection the roof of the third ventricle may be flattened by the often-huge lateral ventricular bodies.

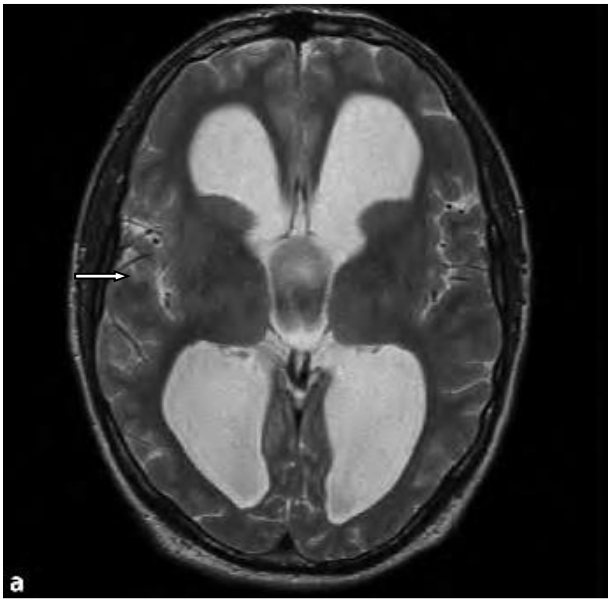

Fig (15): axial T2 MRI image showing Rounding and enlargement of the frontal horns and of the third ventricle (arrows) ***(15).***

iv. Severe dilatation of the bodies and increased height of lateral ventricles:

The degree of dilatation of the lateral ventricles in hydrocephalus is typically notably greater than that occurring secondary to atrophy. The corpus callosum is thinned and bowed forming an arch.

v. Findings in aqueductal stenosis

Severe lateral and third ventricular dilatation with tapering of the third ventricle at the level of the aqueduct and a small fourth ventricle are typical findings of aqueductal stenosis. The frontal horns are ballooned, and

the angle formed by their medial walls (the septal angle) is acute. In atrophy, the frontal horns are typically enlarged but not ballooned, while the septal angle is often obtuse ***(15).***

vi. Enlargement of the fourth ventricle:

This finding assumes the hydrocephalus is communicating. In chronic obstructive hydrocephalus, however, the fourth ventricle may also be enlarged secondary to incisural obstruction created by the enlarged ventricles, dilated temporal horns, and swollen temporal lobes, which tend to herniate into the incisural notch. When present, dilatation of the fourth ventricle can be helpful in establishing the diagnosis of hydrocephalus. However, fourth-ventricular enlargement may be absent or minimal despite the presence of definite hydrocephalus ***(16)***.

Fig (16): Sagittal T2 WI MR shows aqueductal stenosis in distal portion of aqueduct. Note stretched corpus callosum (open arrow) and distended roof and floor of the third ventricles (arrows) ***(14).***

CSF flow void

Flow-void sign is best appreciated in areas of narrowing within the ventricular system such as the aqueduct. The visualization of this effect on routine T2-weighted MR images is not consistent. Sagittal T2-weighted turbo inversion-recovery MR images an aqueductal flow-void sign can be detected in most healthy individuals. If the aqueduct is very narrow (aqueduct area < 1 mm^2) the sign may be very weak or even absent ***(9).*** In most cases, it is sufficient to use Sagittal T2-weighted standard spin echo sequences with 3 mm thickness and 0.5 mm gap, centered on the aqueduct. However, old-fashion dual echo sequence without flow compensation to detect CSF flow are preferred ***(17).***

b. MR Ventriculography

This is additional study determines the site of CSF obstruction in non- communicating hydrocephalus, the functional status of third ventriculostomies, and assesses communication between cysts and the ventricles by injection of gadolinium-based contrast agent to study CSF flow. The technique involves the acquisition of T1-weighted sequences after injection of a gadolinium-based contrast agent into the ventricles (MR ventriculography) or into the lumbar subarachnoid space (MR cisternography). However, accurate diagnosis of a CSF fistula cannot be made unless the high signal of the fistulous communication can be seen in direct continuity with the intracranial subarachnoid space and only few reports showing that the technique is safe and provides accurate information regarding obstruction to CSF flow ***(18).***

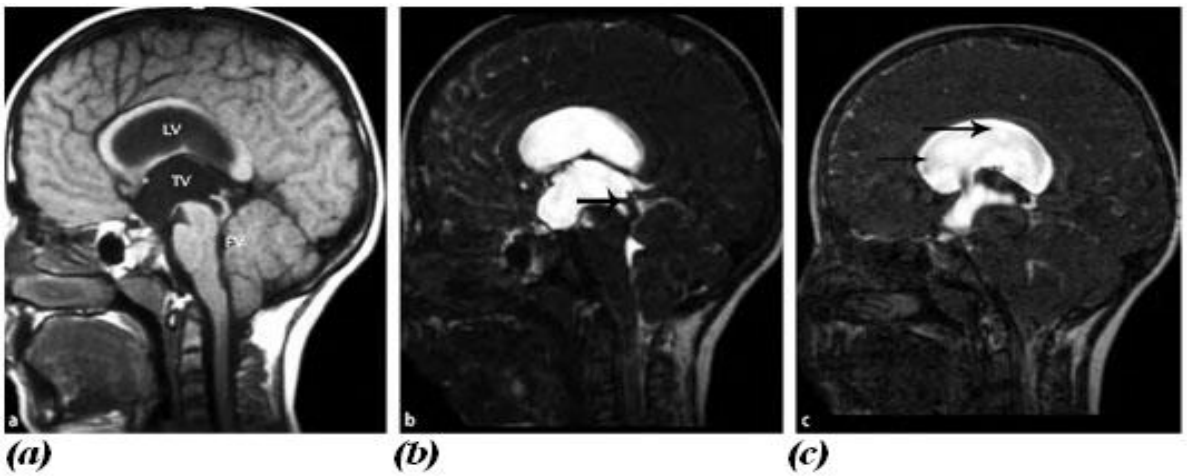

Fig (17): Obstructive hydrocephalus (at the level of the aqueduct of Sylvius). A) T1-weighted imaging showing the fourth ventricles are of usual size, the third and the lateral ventricles are dilated. B) MRCG showing the septum in the aqueduct of Sylvius is seen (arrow). C) MRCG shows heterogeneity of signal from the third and the lateral ventricles cavities due to turbulent CSF flow (arrows) ***(15).***

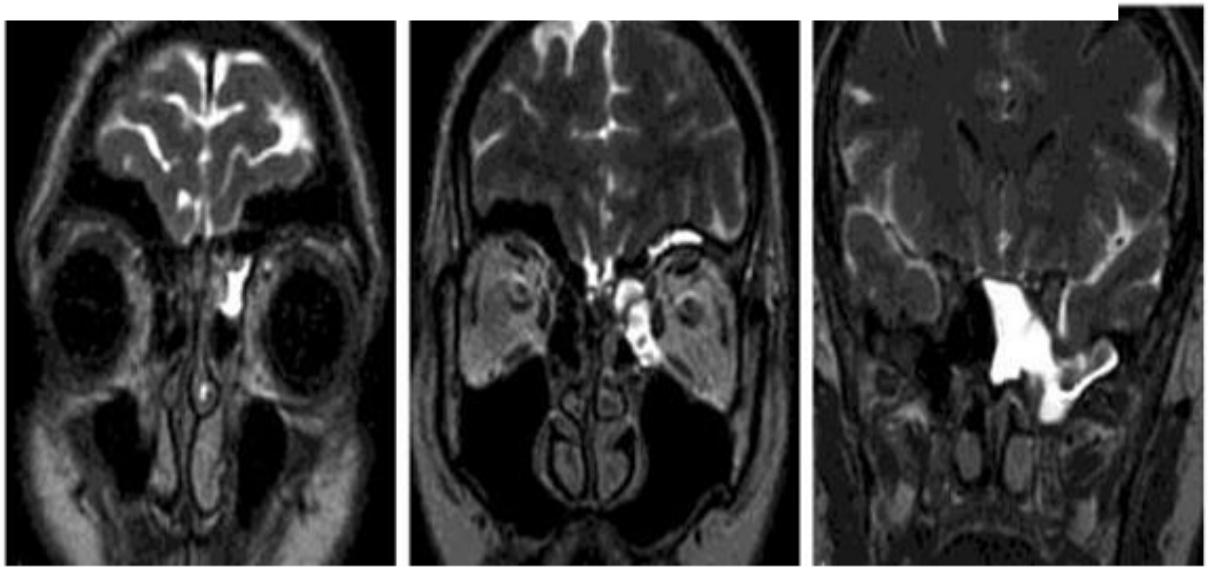

Fig (5): MRCG shows nasal CSF leak &two fistulas in ethmoid & sphenoid bones ***(15).***

Clinical application of CSF flowmetry in various neurological conditions

Phase-contrast MRI can be used for quantitative assessment of CSF flow, in which measurements such as flow velocity and volume are used to diagnose conditions and direct care in the appropriate patients. In addition, phase-contrast MRI enables qualitative assessment of CSF circulation (ie, bulk flow) and back-and forth motion (ie, pulsatile flow). One of the most widely used applications of CSF flow imaging is functional assessment of normal pressure hydrocephalus (NPH). Hyperdynamic flow of CSF is seen when there is enlargement of the ventricular system in the absence of or out of proportion to the sulcal enlargement (ventriculosulcal disproportion). Patients with NPH who have hyperdynamic CSF flow respond better to ventriculoperitoneal shunt placement than do patients with normal or decreased flow ***(18)***.

1. Normal pressure hydrocephalus

Normal pressure hydrocephalus (NPH) is a type of communicating hydrocephalus (without obstruction of CSF outflow) first described by Hakim and Adams in 1965. It is an idiopathic condition, mostly affecting elderly patients with a clinical triad of gait disturbance, dementia, and urinary incontinence (**19**). Since then, NPH has been the subject of numerous studies which revealed that up to 10% of people with dementia have been suspected to have NPH and may profit from treatment. (**19**).

Despite the development of medical guidelines, diagnostic imaging methods, and extensive studies, its poor clinical manifestation (complete triad of symptoms is merely present) and non-specific changes in radiological findings (the first and the only alteration is often enlarged ventricles) proves that NPH remains a diagnostic problem. Typically, a long asymptomatic period with only slight changes in MRI images are the more common presentation. Nevertheless, patients suffering from secondary NPH (following a subarachnoid hemorrhage) develop symptoms earlier than patients with primary (idiopathic) NPH. Magnetic resonance assessment of the brain is crucial in the NPH diagnostic procedure, revealing several morphological and functional alterations. Typical morphological findings include ventriculomegaly, narrow callosal angle (< 90°), periventricular high signal on T2-weighted sequences, and tight sulci in convexities of the cerebral hemispheres. Functionally, a flow rate of > 24.5 mL/min is 95% specific for NPH and aqueductal flow void artefact is diagnostic ***(20).***

Due to technological advances and widespread accessibility of PC-MRI, it superseded spin echo images. In 1996, It was proposed that an aqueductal stroke volume > 42 μl as a cut off value above which patients with NPH were thought to benefit from VPS placement Since then, the subject has been extensively studied as a promising method for non-invasive assessment of CSF flow with ambiguous results. It was proposed that CSF flow > 18 ml/min as a cut-off point in the PC-MRI ***(8)***. It was proved that the peak systolic velocity in the aqueduct strongly correlates with a positive clinical response to shunting . Moreover, It was combined PC-MRI with a high-volume CSF tap test to identify patients with NPH who would qualify for a VPS ***(20).***

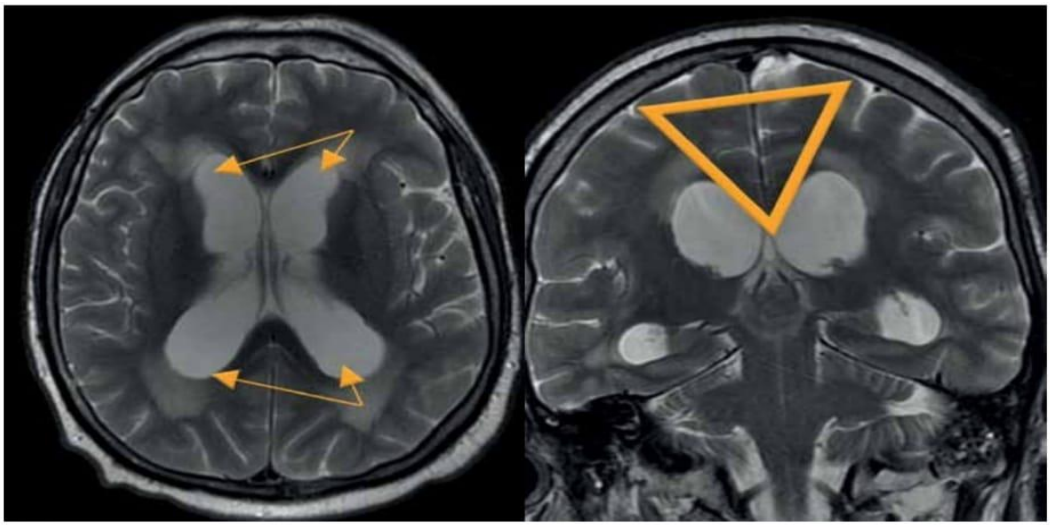

Figure 6 Morphological changes in normal pressure hydrocephalus. Ventriculomegaly with pronounced dilatation of the frontal and temporal horns (left image) and a narrow callosal angle (right image) ***(2).***

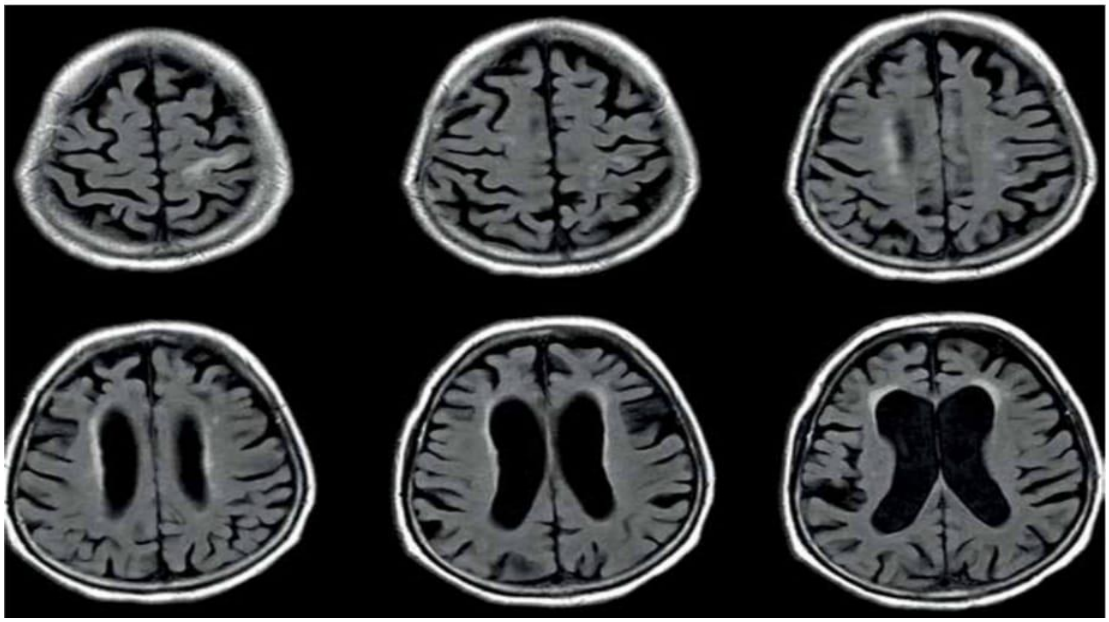

Figure 7 Periventricular high T2 signal on T2-weighted imaging. Example of magnetic resonance imaging findings in patients with normal pressure hydrocephalus. ***(2).***

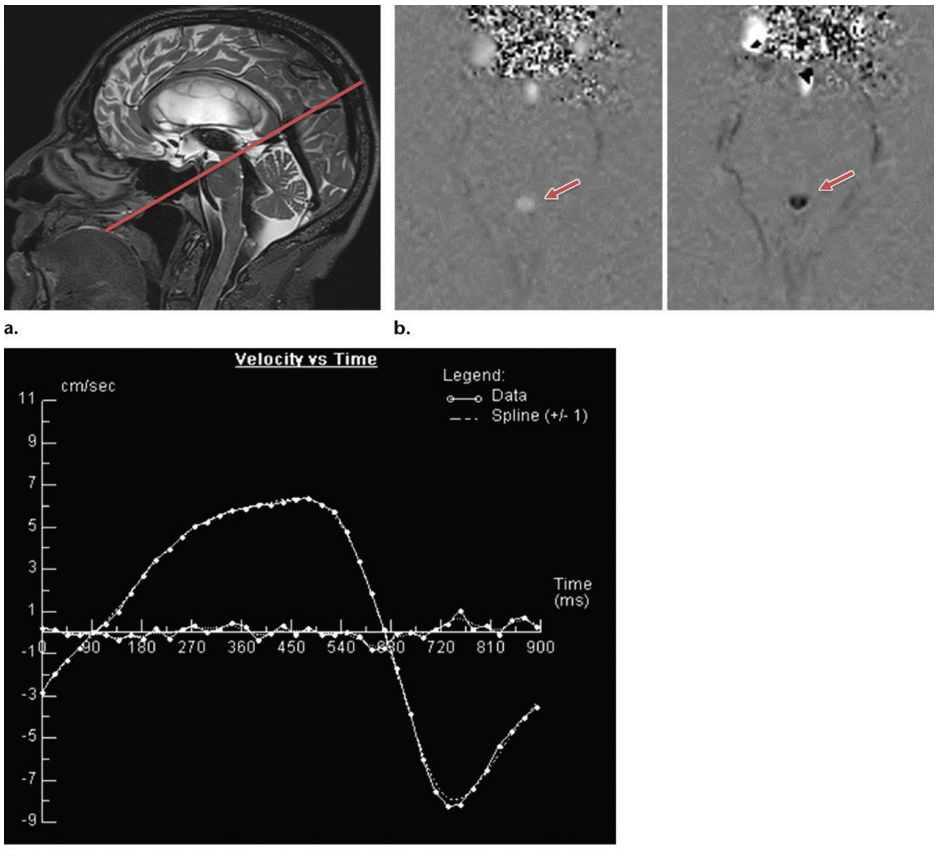

Figure 8. Clinically suspected NPH. (a) Midsagittal T2-weighted high-spatial-resolution 3D fast spin-echo MR image excludes anatomic obstruction. Signal void is also seen spanning the third and fourth ventricles and reflects high velocities. A plane for phase-contrast imaging (red line) is prescribed perpendicular to the cerebral aqueduct, yielding axial phase-contrast images. (b) The axial phase-contrast images show high (left) and low (right) signal intensity (arrow) in the cerebral aqueduct, reflecting to-and-fro pulsatile CSF flow. (c) Volumetric CSF flow curve through the aqueduct shows nearly sinusoidal flow during a cardiac cycle, demonstrating to-and-fro CSF flow (13). In this patient, the qualitative assessment of high flow on the high-

spatial resolution images (a and b) was combined with a measured aqueductal CSF stroke volume greater than 50 .L to corroborate the clinical diagnosis of NPH. **(3)**

2. Brain atrophy

Ventricular dilatation is the main finding in brain atrophy. It is always mild but symmetrical. Ventricular dilatation is proportional to the widening of the subarachnoid spaces. This change is better assessed on T1 WI MRI as an abnormal high signal intensity white matter progressively increasing with age as a result of ischemic changes. It may be seen in both deep and periventricular white matter regions. CSF flow studies help to differentiate it from NPH by demonstrating a hypodynamic flow curve ***(21).***

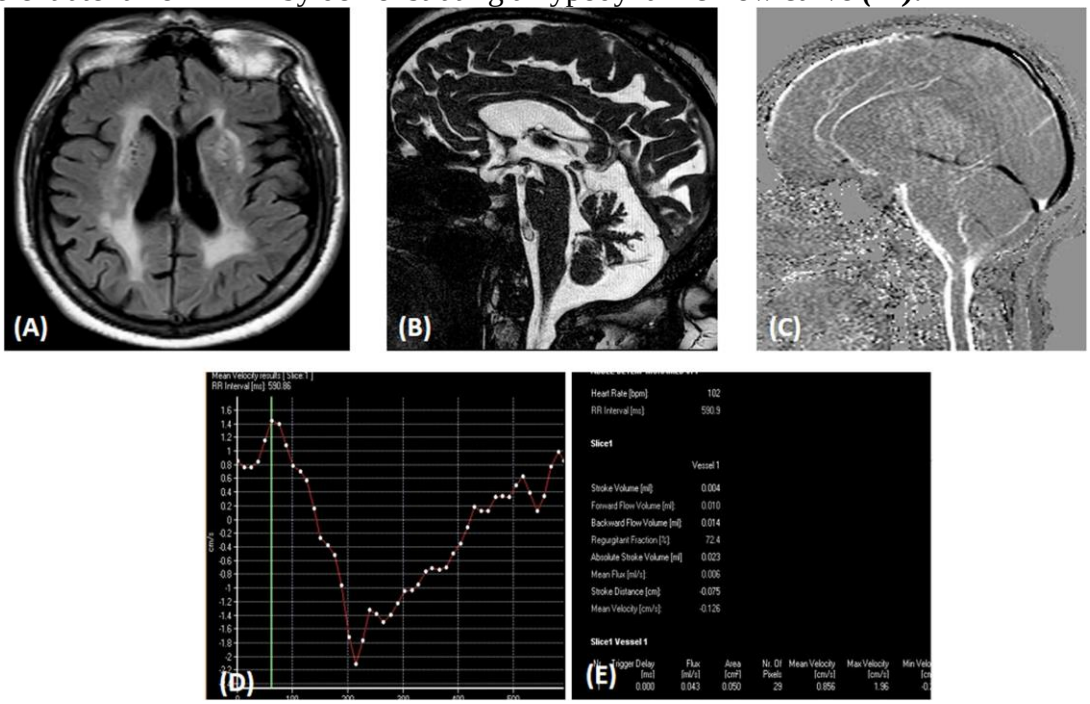

Fig.9 ; 24 Female patient presented with gait disturbance and difficult urinary control. a MRI axial FLAIR, mild dilatation of the lateral ventricles, and white matter abnormal hyperintensity representing ischemic changes. b 3D DRIVE image showing patent normal aqueduct. c Sagittal phase image in systole showing CSF flow in the aqueduct of Sylvius as shades of white. d Velocity time curve showing CSF in both diastole and systolic PDV = 1.4 cm/s, PSV = 2.2 cm/s, and Vmax = (1.4 + 2.2)/2 = 1.8 cm/s. e CSF flow curve associated table, Forward flow volume = 10 μl, and backward flow volume = 14 μl, and so the SV = (10 + 14)/2 = 12 μl/cycle. Aqueduct area = 0.05 cm2. So the maximum flow was calculated as follows: maximum flow = 1.8 × 0.05 = 0.09 cm3/s. Diagnosis is hypodynamic CSF flow consistent with brain atrophy (***22***).

Ventriculoperitoneal (VP) shunts

VPS is a procedure used in the management of various neurological conditions with the aim to drainage any excessive amount of CSF and avoid excessive intracranial pressure. In this procedure, an inflow catheter with a pressure-sensitive valve is inserted into the ventricles, and an outflow catheter is located in the peritoneal cavity. Unidirectional, pulsatile flow with a specific velocity and the patency of the shunt can be evaluated with PC-MRI with VENC values usually chosen above 2-5 cm/s. Although there are other methods to visualize patency, such as flow void artefact on conventional sequences or Time-SLIP sequence, PC-MRI is the only quantitively method available. PC-MRI has not only been proven to assess patency (as evidenced by unidirectional brighter signal within the shunt, but also has been evaluated as a potential prediction method of postsurgical outcome. Nevertheless, negative results were still found in patients who underwent VPS. Finding a proper reliable biomarker of a positive surgical outcome requires further studies and investigations ***(2).***

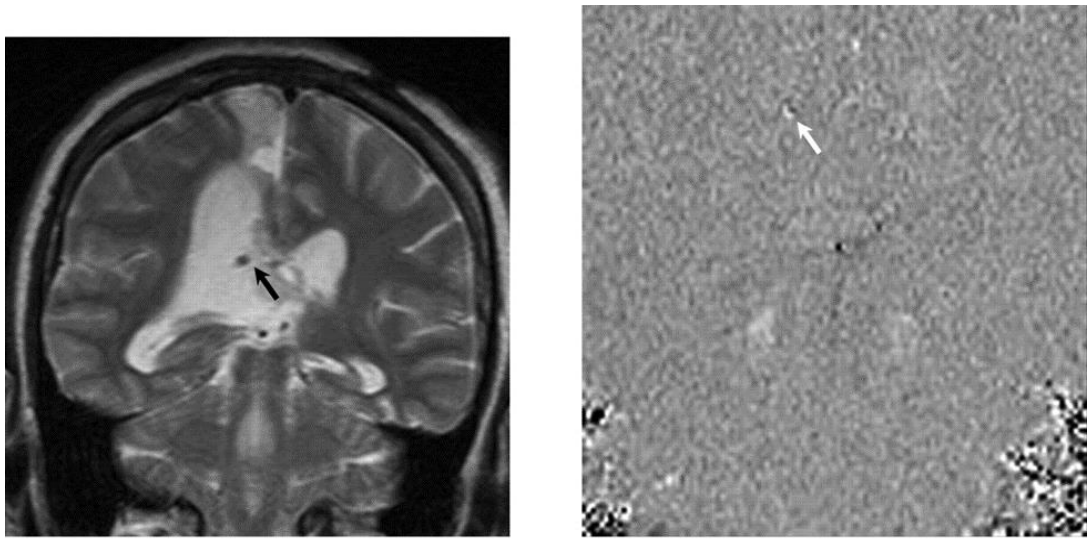

(a) (b)

Figure 10 : A 34-year-old female patient with a ventriculoperitoneal shunt inserted for obstructive hydrocephalus. (a) Coronal T2 weighted MRI shows the ventriculoperitoneal shunt (black arrow) within the right ventricle. (b) Coronal cerebrospinal fluid flow MRI demonstrates brighter signal intensity (white arrow) than the background, suggesting patency at the site of the shunt. This flow pattern is consistent with the one-way flow in the ventriculoperitoneal shunt. (**23)**

3. Chiari 1 malformation

The Chiari 1 malformation, also known as the Arnold–Chiari malformation, is caudal displacement of the cerebellar tonsils through the posterior foramen magnum. The suggestive symptoms of this malformation include headaches, dizziness, ataxia, fainting with a cough, weakness or numbness, episodic aural fullness, tinnitus and vertigo. Routine MRI sequences are the imaging modality of choice for assessing Chiari I malformations (best seen in sagittal plane). The cerebellar tonsils are pointed, rather than rounded and referred to as peg-like. A measurement is then drawn perpendicular to this plane (from the anterior to the posterior margin of the foramen magnum / plane of foramen magnum); between it and the tip of the cerebellar tonsils, either in the midsagittal image or an adjacent parasagittal image, wherever the tonsils are most low lying. This finding may present with or without syringomyelia. CSF flow studies using PC MRI are now routinely used to determine the severity of CSF flow disturbance and to assess the flow surrounding the cervicomedullary junction. The degree of CSF flow disturbance has been shown to correlate with severity and development of clinical symptoms ***(24)*** .

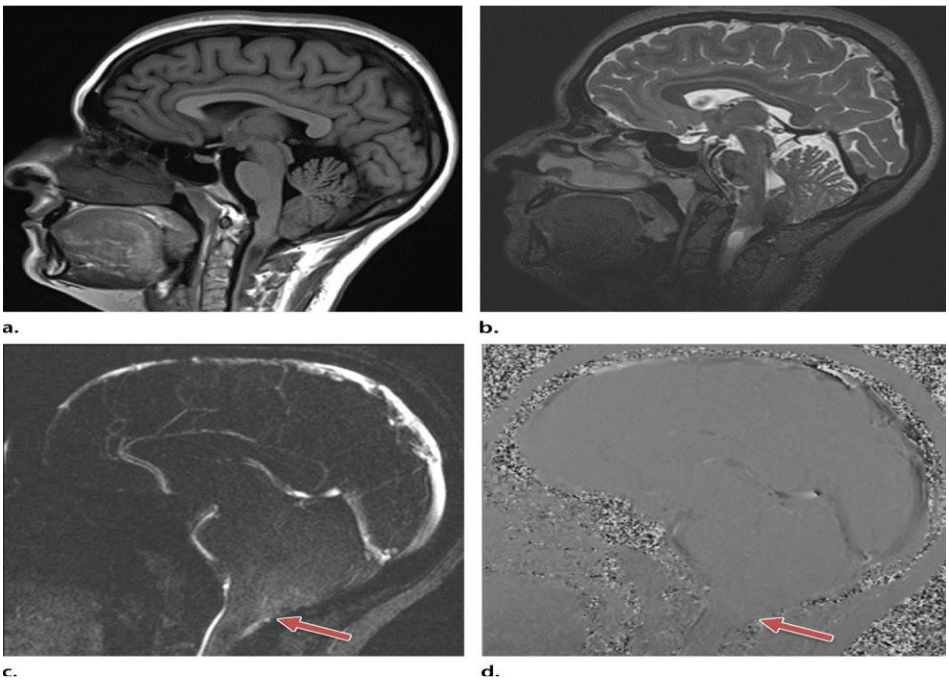

Figure 11. Chiari I malformation with restricted CSF flow. (a) Parasagittal T1-weighted MR image shows cerebellar tonsillar ectopia and low T1 signal intensity in the cervical spinal cord. (b) Parasagittal T2-weighted high spatial-resolution 3D fast spin-echo MR image shows high T2 signal intensity in the cervical cord, compatible with a syrinx. (c, d) Parasagittal magnitude (c) and phase (d) phase-contrast images show a loss of communication between the cisterna magna and posterior cervical subarachnoid space (arrow). Preserved to-and-fro CSF flow is seen in the prepontine cistern. **(3)**

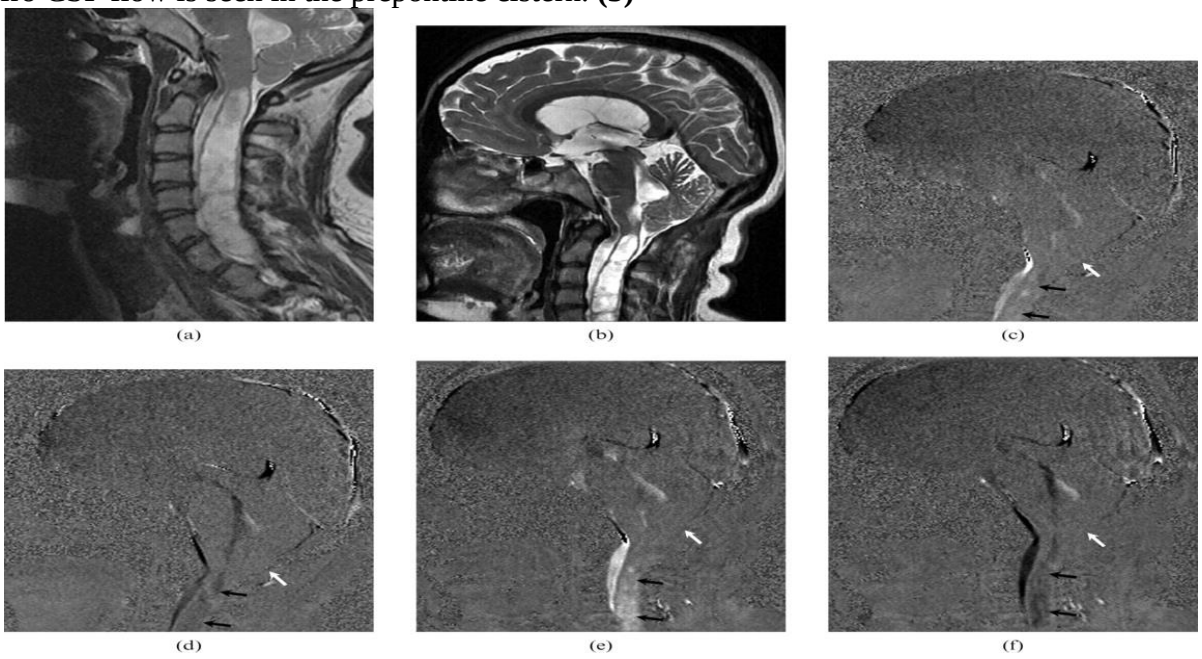

Figure 12: A 24-year-old female with the diagnosis of Chiari 1 malformation presented with sub-occipital headache. (a) Pre-operative and (b) post-operative sagittal T2 weighted MRI show a large syrinx in association with cerebellar tonsillar ectopia. (c, d) Pre- and (e, f) post-operative cerebrospinal fluid (CSF) flow MRI show no association between cervical subarachnoid space and cisterna magna (white arrow). No symptomatic improvement was observed after the surgery. Both pre-operative and post-operative CSF flow MRI (c–f) show pulsatile CSF flow in the syrinx (black arrows). (23**)**

4. Arachnoid cyst

Although there has been considerable controversy regarding the exact indications for surgical treatment of asymptomatic arachnoid cysts, patients with symptomatic cysts i.e., cyst causing seizures, hydrocephalus, increased intracranial pressure, or neurological impairment should be treated. Preoperative determination of whether an arachnoid cyst is communicating to the CSF spaces is important step in pre-operative evaluation. Moreover, discrimination between normal CSF spaces and intracranial cysts may not always be evident with anatomical imaging and may need to be further clarified with flow studies. CSF flow patterns specific to each entity and PC MRI improves diagnostic confidence when differentiating communicating versus non-communicating arachnoid cysts from posterior fossa cystic malformations ***(25)*.**

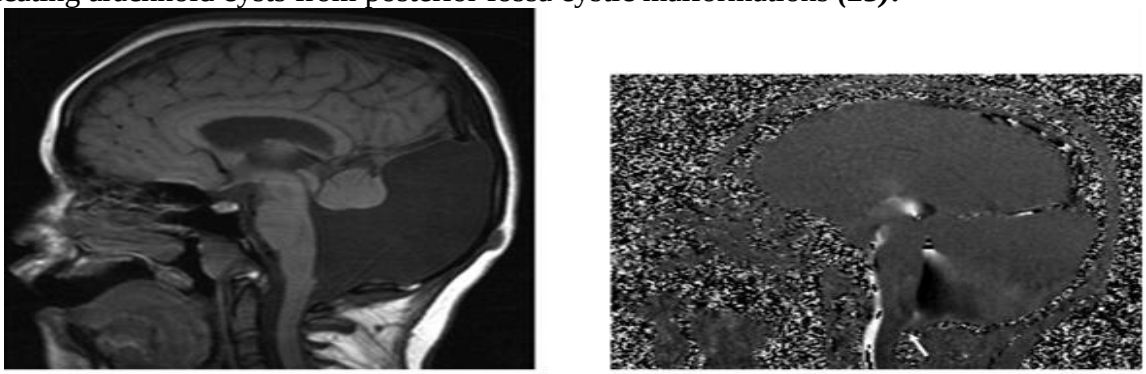

Figure 13 : A 14-year-old female with Dandy-Walker malformation. (a) T1 weighted sagittal image demonstrates the dilated fourth ventricle associated with the posterior fossa cystic lesion, elevation of the tentorium, widening of the posterior fossa and dysgenesis of the vermis. (b) Cerebrospinal fluid (CSF) flow MRI shows no communication between the cyst and the posterior cervical subarachnoid space (arrow), and hyperdynamic CSF flow through the aqueduct into the cyst produces turbulent flow within the cyst. (**23)**

5. Other clinical applications

Syringomyelia

Various theories on the pathophysiology of syringomyelic cysts have been reported, but the most popular is that formation and extension of such cysts result from an obstruction of spinal CSF pathways. Syringomyelic cysts are associated with several conditions including Chiari 1 malformation, spinal trauma, spinal cord tumors, and arachnoiditis. The detection of pulsatile CSF flow within the cystic cord lesion is both predictive of subsequent enlargement and may help discriminate a cyst from a myelomalacia. CSF flow imaging can provide direct evaluation, follow-up, and postoperative evaluation in patients with syringomyelic cysts ***(26)***.

Neuroendoscopic third ventriculostomy

Neuroendoscopic third ventriculostomy (NTV) is increasingly used alternative treatment for obstructive hydrocephalus. It has become a common neuroendoscopic procedure aiming to restore the pulsatile bidirectional CSF motion. Indications for NTV remain controversial. Although it is an internal CSF diversionary procedure best suited to non-communicating hydrocephalus, it has had some unexplained success in communicating hydrocephalus with low morbidity and high success rates. ***(26)***.

A group of image parameters have been assessed to evaluate the permeability of the NTV, including ventricular size changes, flow void signal intensity and MR patency, by using cine PC MR. PC flow-sensitive MRI techniques offer more physiological data than structural MRI and qualitatively assess the patency of the ventriculostomy. In addition, stroke volume measurements within the ventriculostomy provide functional information about its patency ***(2).***

Brain masses like tumors may lead to features of obstructive hydrocephalus and the operated tumors had post operative conventional MRI changes of evaco-dilatation of the ipsilateral ventricle , may lead to increase of CSF pressure that can be evaluated by CSF flow parameters to determine effect of tumors on CSF pressure **(27)**.

References

1. Saloner D. The AAPM/RSNA physics tutorial for residents. An introduction to MR angiography. Radiographics 1995; 15: 453-465.
2. Adrian Korbecki , Anna Zimny , Przemysław Podgórski , Marek Sąsiadek, Joanna Bladowska Imaging of cerebrospinal fluid flow: fundamentals, techniques, and clinical applications of phase-contrast magnetic resonance imaging 2019 . Doi : 10.5114 / pjr. 2019.86881 . PMID : 31482996.
3. David T. Wymer, MD ,Kunal P. Patel, MD William F. Burke III, MD Vinay K. Bhatia, MD Phase-Contrast MRI: Physics, Techniques,and Clinical application 2020 . PMID: 31917664 ,
4. Horie T, Kajihara N, Matsumae M, et al. Magnetic Resonance Imaging Technique for Visualization of Irregular Cerebrospinal Fluid Motion in the Ventricular System and Subarachnoid Space. World Neurosurg 2017; 97: 523-531.
5. Pelc NJ, Herfkens RJ, Shimakawa A, Enzmann DR. Phase contrast cine magnetic resonance imaging. Magn Reson Q 1991;7 ; 229-254.
6. Kasapas K, Varthalitis D, Georgakoulias N et al. (2015): Hydrocephalus due to Membraneous Obstruction of Magendi's Foramen. jkns., 57;1:68-71.
7. Halperin JJ., Roger Kurlan: Practice guideline: Idiopathic normal pressure hydrocephalus: Response to shunting and predictors of response. American Academy of Neurology, 2015.
8. Luetmer PH, Huston J, Friedman JA, et al. Measurement of cerebrospinal fluid flow at the cerebral aqueduct by use of phase-contrast magnetic resonance imaging: technique validation and utility in diagnosing idiopathic normal pressure hydrocephalus. Neurosurgery 2002; 50: 534.
9. Schroeder HWS , Schweim C, Schweim KH , ET AL ; analysis of aqueductal cerebrospinal fluid flow after endoscopic aqueductoplasty by using cine phase-contrast magnetic resonance imaging .J. Nuerosurg 2000*93 ;* - , pp 237-244
10. Albright al. hydrocephalus in children in ; Rengachary SS , Wilkins RH. Princibles of neurosurgery . London ; Wolfe, 1994 ; chapter 6.
11. Black P MCl , Matsumae M. hydrocephalus in adults in Rengachary SS , Wilkins RH. Princibles of neurosurgery . London ; Wolfe, 1994 ; chapter 7.
12. Whitelaw A, Kennedy CR , Brion LP : Diuretic therapy for newborn infants with postthemorrhagic ventricular dilataion . Cochrane database syst rev. 2001: CD 002270 (PMC free article (Pub Med).
13. Mori K. current concept of hydrocephalus : evaluation of new classification . Childs Nsyst. 1995 ; 11 523-531.
14. Blaser SI , Osborn AAGG , Salzman KL ,et al : congenital malformation s in Diagnostic Imaging brain , 1st edition , Chiari 2 2004 ; pp I-1-12 :16.
15. Kornienko VN, Pronin IN ; hydrocephalus in Diagnostic Neuroradiology , 2009 , pp 919-933.
16. Haaga JR , Lanzieri CF , Sartoris DJ , Zeerhouni EA : computed tomography and magnatic resonance imaging of the whole body , 2004 ; pp 328-334.
17. Greitz D. Radiological assessment of hydrocephalus: new theories and implications for therapy. Neurosurg Rev. 2004 ; pp 27 145-165.
18. Siebner HR , von Einsiedel H, Conrad B : - Magnetic resonance ventriculography with gadolinium DTPA (1997) neuroradiology 39 , 418-422.
19. Adams RD, Fisher CM, Hakim S, Ojemann RG, Sweet WH. Symptomatic Occult Hydrocephalus with Normal Cerebrospinal-Fluid Pressure. N Engl J Med 1965; 273: 117-126.
20. Kitagaki H, Mori E, Ishii K, et al. CSF spaces in idiopathic normal pressure hydrocephalus: morphology and volumetry. AJNR Am J Neuroradiol 1998; 19: 1277-1284.
21. Barkhof F, Kouwenhoven M, Scheltens P, Sprenger M, Algra P & Valk J: Phase-contrast cine MR imaging of normal aqueductal CSF flow. Effect of aging and relation to CSF void on modulus MR. Acta Radiol. 1994, 35: 123-130.
22. Ahmed Mohamed Tawfik , Lamiaa Elsorogy , Rabab Abdelghaffar ,Ayman Abdel Naby ,Ibrahim Elmenshawi ; Phase-Contrast MRI CSF Flow Measurements for the Diagnosis of Normal-Pressure Hydrocephalus: Observer Agreement of Velocity Versus Volume Parameters 2016.
23. Battal B, Kocaoglu M, Bulakbasi N, Husmen G, Tuba Sanal H, Tayfun C (2011) Cerebrospinal fluid flow imaging by using phase-contrast MR technique. Br J Radiol 84:758–765
24. M Panigrahi 1, B Praveen Reddy, A K Reddy, J J M Reddy ; CSF flow study in Chiari I malformation . PMID: 15085382 , Childs Nerv Syst . 2004 May;20(5):336-40.
25. Karl T. Hoffmann, a Norbert Hosten,a Bernd U. Meyer,a Simone Röricht,a Christian Sprung,a Johann Oellinger,a Matthius Gutberlet,a and Roland Felixa ; CSF Flow Studies of Intracranial Cysts and Cyst-like Lesions Achieved Using Reversed Fast Imaging with Steady-State Precession MR Sequences . AJNR Am J Neuroradiol. 2000 Mar; 21(3): 493–502.
26. Brugieres P, Idy-Peretti I, Iffenecker C, et al. CSF flow measurement syringomyelia. AJNR Am J Neuroradiol 2000; 21: 1785-1792.
27. Merve Gulbiz Kartal & Oktay Algin : Evaluation of hydrocephalus and other cerebrospinal fluid disorders with MRI: An update Insights into Imaging volume 5, pages531–541 (2014).